IJCRT.ORG ISSN : 2320-2882

INTERNATIONAL JOURNAL OF CREATIVE RESEARCH THOUGHTS (IJCRT)

An International Open Access, Peer-reviewed, Refereed Journal

# PERFORMANCE ANALYSIS OF $SiO_2$ BASED MICRORING RESONATOR USING FINITE-DIFFERENCE TIME-DOMAIN (FDTD)

[1]Kuldeep Singh, [1]Aditya Malhotra, [1]Amit Kumar, [1]Anukriti Jaiswal

[1]Department of Electronics and Communication Engineering

[1]Galgotias College of Engineering and Technology, Greater Noida, Uttar Pradesh, India

Abstract: This work analyzes the performance of a silicon photonic micro-ring resonator using the Finite-Difference Time-Domain (FDTD) method. Micro-ring resonators are critical components for implementing photonic computation and communication circuits in next-generation systems. Their resonance properties are fundamental to silicon photonic technology and require detailed study for effective circuit and system design. The analysis focuses on resonant characteristics for ring radii ranging from 2 μm to 20 μm, considering a waveguide group index of 3. Results demonstrate a significant dependence of device quality on ring size. A resonator with a 2 μm radius exhibits a Q-factor of approximately 83.3, whereas a 20 μm radius resonator achieves a Q-factor of 393.7 under the specified conditions.

**Index Terms** – $SiO_2$, Microring resonator, FDTD.

## I. INTRODUCTION

Future computing systems face inherent limitations in processing speed and capacity as traditional CMOS-based semiconductor technology approaches its performance ceiling. To sustain performance scaling anticipated by Moore's law, alternative research avenues are essential. Silicon photonics emerges as a promising solution to overcome the constraints of conventional CMOS electronics. Optical technologies offer proven advantages in reliability and performance efficiency.

Crucially, photonic devices and systems enable significantly higher data transmission speeds and processing bandwidth compared to electronic counterparts. Optical signals propagating through silicon waveguides avoid the capacitive charging delays inherent in electronic circuits. Furthermore, photons can traverse waveguides without mutual interference and are largely unaffected by electromagnetic radiation, unlike electrons. These inherent benefits make photonic data transmission, computation, and storage highly attractive for next-generation high-performance technologies [1-4].

Numerical analysis of ring resonators can be performed via mathematical modeling or the FDTD technique. The FDTD method solves Maxwell's time-dependent equations directly. Its time-domain approach is particularly advantageous for capturing transient reflection behavior and radiation effects, aspects often omitted in alternative waveguide analysis methods. Consequently, this paper employs FDTD to investigate the resonant filter characteristics [5-6]. While the tunneling effect provides a basis for non-resonant lossless optical filters, their performance capabilities are inherently limited and independent of specific refractive index sequences [7]. The coupling of energy between optical waveguides and ring resonators remains an active research topic.

Interest has intensified due to its potential for enabling vital functions in optical fiber communication systems [8]. Given the importance of micro-ring resonators in silicon photonics, this research focuses on analyzing their quality factor (Q-factor) based on resonance theory. The findings are intended to support the design of photonic circuits and systems for advanced computing and communication applications.

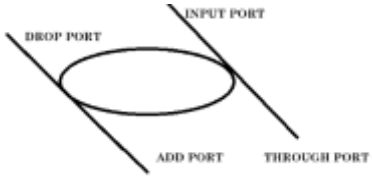


Fig. 1 Schematic of single micro ring resonator

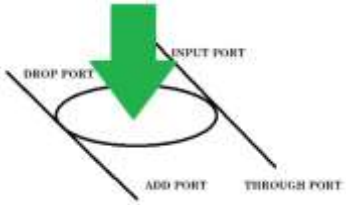


Fig. 2 Optical Pumping in Micro Ring Resonator

## II. Optical Ring Resonator Fundamentals

An optical ring resonator consists of waveguides where at least one forms a closed loop coupled to input/output light paths. Its operation principles are analogous to whispering gallery phenomena but utilize light waves governed by constructive interference and total internal reflection. When resonant-wavelength light enters the loop via the input waveguide, it circulates and intensifies through multiple round trips due to constructive interference. The amplified output couples to a detector waveguide. Since only specific wavelengths resonate within the loop, the device functions as an optical filter. Multiple interconnected ring waveguides can further create add/drop filter configurations [22].

### 2.1. Coupling Dynamics

When the waveguide and ring are in proximity, optical power transfers between them. Neglecting transmission losses, scattering, and back-reflection over the coupling length, the interaction is described by:

$$\begin{bmatrix} E_t \\ E_{r1} \end{bmatrix} = \begin{bmatrix} t & K \\ -K^* & t^* \end{bmatrix} \begin{bmatrix} E_i \\ E_{r2} \end{bmatrix} \quad (1)$$

Here, t is the self-coupling coefficient (fraction of field amplitude remaining in the original waveguide), and κ is the cross-coupling coefficient (fraction transferred between waveguides). In addition, the $E_i$ input field has a complex mode dimension and through the $E_t$ port, the output mode has a complex mode dimension. Complex field amplitude $E_i$ (input), $E_t$ (through port), $E_{r1}$ and $E_{r2}$ are normalized so that their squared amount corresponds to modal power [18, 23]. For lossless coupling,

$$|K|^2 + |t|^2 = 1 \quad (2)$$

### 2.2. Spectral Characteristics

The Free Spectral Range (FSR) defines the wavelength separation between consecutive resonances. The resonance condition $\omega T_R = m2\pi$ (where $T_R$ = round trip time, m= integer) yields frequency domain FSR

$$FSR_{frequency} = \omega_2 - \omega_1 = \frac{2\pi}{T_r} = \frac{2\pi c}{Ln_{eff}} \quad (3)$$

FSR in terms of wavelength,

$$FSR_{wavelength} = \frac{\lambda^2}{Ln_{eff}} \quad (4)$$

Here, the optical path length of ring is L (L = 2πR) and is an effective refractive index waveguide is $n_{eff}$. If the wavelength dependency of the effective index cannot be ignored, then the group refractive index ($n_g$) can be used instead of the effective index (neff), whenever appropriate [18, 23].

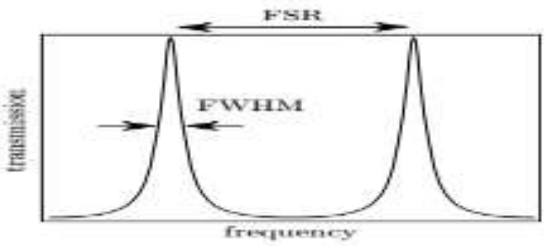


Fig. 3 The transmission spectrum showing FSR and FWHM [20]

### 2.3. Resonance Bandwidth and Quality Factor

The Full Width at Half Maximum (FWHM) denotes the resonance bandwidth at 50% transmission (3-dB point), as illustrated in Figure 3. For an add-drop resonator with identical couplers (t1=t2=t) and round-trip amplitude transmission a:

$$FWHM = \frac{\lambda^2}{\pi L n_g} \frac{1-at}{\sqrt{at}} \quad (5)$$

The Quality factor (Q) quantifies resonance sharpness as the ratio of stored energy to dissipated energy per cycle:

$$Q = \omega_o \frac{\text{Stored Energy}}{\text{Power Loss}} \quad (6)$$

Equivalently, in terms of spectral parameters [18, 23]:

$$Q = \frac{\lambda_{res}}{FWHM} = \frac{\pi L n_g}{\lambda} \frac{\sqrt{at}}{1-at} \quad (7)$$

## III. LITERATURE SURVEY

| S. No. | Reference | Content evaluated | Observation |
|---|---|---|---|
| 1 | [9] | The condition of critical coupling is a fundamental property of waveguides coupled to resonators. | Wavelength-selective switching |
| 2 | [10] | Coupling among waveguides and resonators. | Speed of coupling |
| 3 | [11] | The silicon-on insulator (SOI) material system is ideally suited for nanophotonic waveguides. | The waveguides will be susceptible to phase fluctuations due to small changes in waveguide geometry. |
| 4 | [12] | The sum of the energies from two photons is sufficient to excite an electron across the indirect band-gap of silicon. | The reduction in the carrier lifetime from ion implantation reduce loss from free carriers. |
| 5 | [13] | Balanced SCISSOR configuration, | Effect on delay by a greater number of microrings. |
| 6 | [14] | When the waves in the loop build up a round-trip phase shift that equals an integer times 2π, the waves interfere constructively and the cavity is in resonance. | Most of the aspects of silicon ring resonators. |
| 7 | [15] | If wavelength is increased then the amplitude in the ring is larger than that from the input due to the constructive interference of light in the loops. | Simulation time is long but method is easy. |
| 8 | [16] | As a four-port device, there are two possible output ports, denoted as “Drop” and “Through”, respectively | The spectrums of the proposed structure exhibit sharp asymmetric |
| 9 | [17] | SOI is the common material used in optical resonators. | The larger size of optical cavities leads to greater transmission loss, which is not conducive to improvement of the quality factor |
| 10 | [18] | Analysis of the resonance behaviour of a silicon photonic micro-ring resonator | Done with single waveguide |
| 11 | [19] | Structure compatible with most of today’s CMOS-based silicon photonics technology platforms. Multiple rings will impose additional requirements. | Not possible to reduce the roundtrip length of the ring indefinitely. This will complicate the tuning scheme |

## IV. DESIGN OF MICRORING RESONATOR

The micro ring resonator has been made on FDTD Mode Solution Tool and is shown in Fig. 4. The structure is made on $SiO_2$ (glass) Palik base. The Gaussian source is provided to the input port while the results are taken from the Through port and Drop port. The structure is made by having two parallel rectangular waveguides with a circular waveguide in between them as well as frequency and time monitors are connected to through port and drop port as shown in Fig. 4. The wavelength range taken for this design is from 1.5µm to 1.6 µm. The design parameters of micro ring resonator are as shown in Table 1.

Table 1 Parameters of Micro Ring Resonator

| S. No. | Parameter | Value | Unit |
|---|---|---|---|
| **1.** | Coupling Length | 0 | µm |
| **2.** | Gap | 0.1 | µm |
| **3.** | Radius | 2-20 | µm |
| **4.** | Refractive Index | 3 | |
| **5.** | Material | Si - Palik | |
| **6.** | Base Width | 0.4 | µm |
| **7.** | Height | 0.18 | µm |
| **8.** | Wavelength | 1.5-1.6 | µm |

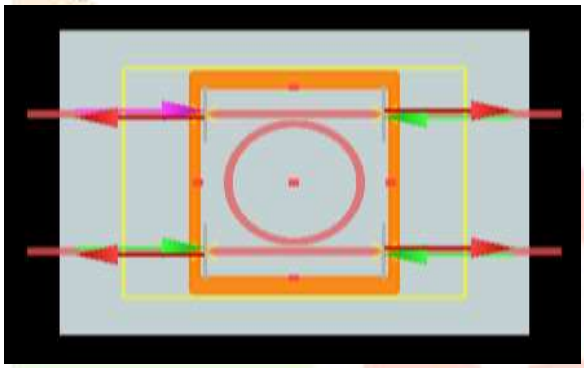

Fig. 4 Simulated design of single ring resonator in FDTD [21]

## IV. RESULTS AND DISCUSSION

The simulated results of Micro Ring Resonator has been shown in Fig 5-12.

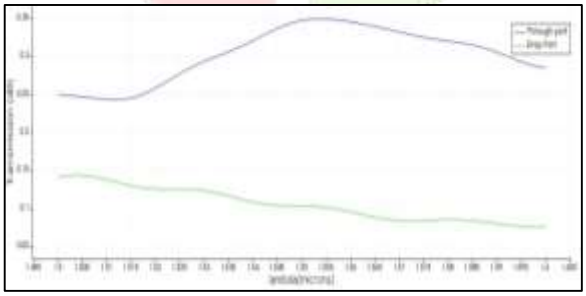

Fig. 5 Transmission plot for radius 2 µm and index=3

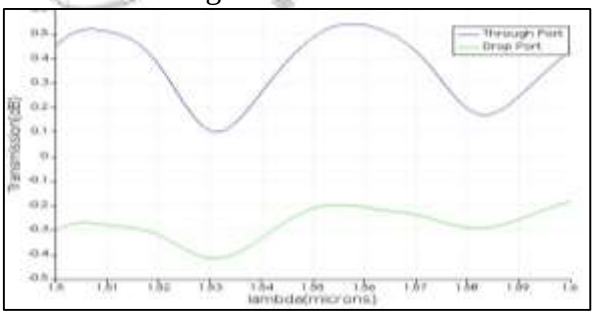


Fig. 6 Transmission plot for radius 4 µm and index=3

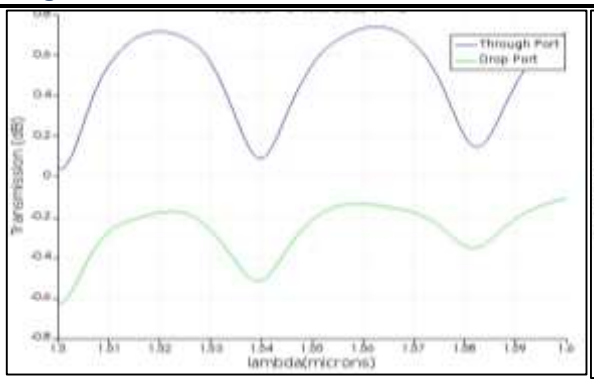


Fig. 7 Transmission plot for radius 5 μm and index=3

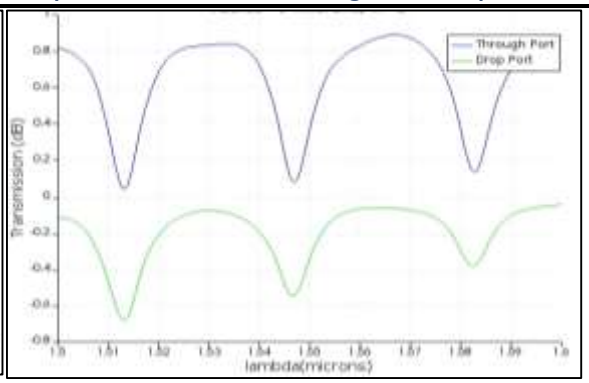


Fig. 8 Transmission plot for radius 6 μm and index=3

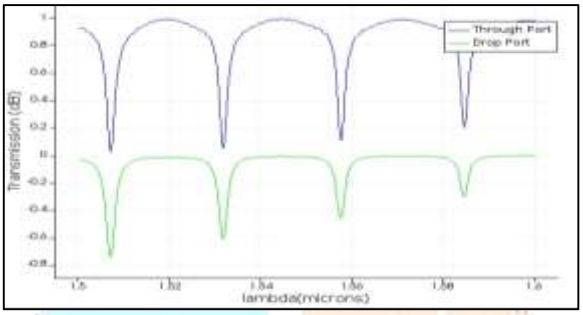


Fig. 9 Transmission plot for radius 8 μm and index=3

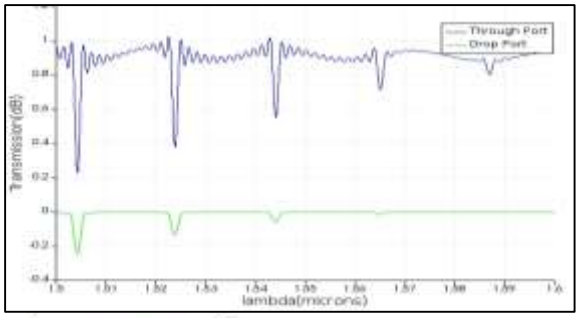


Fig. 10 Transmission plot for radius 10 μm and index=3

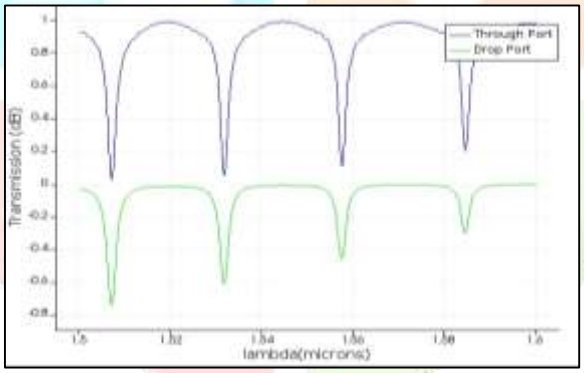


Fig. 11 Transmission plot for radius 15 μm and index=3

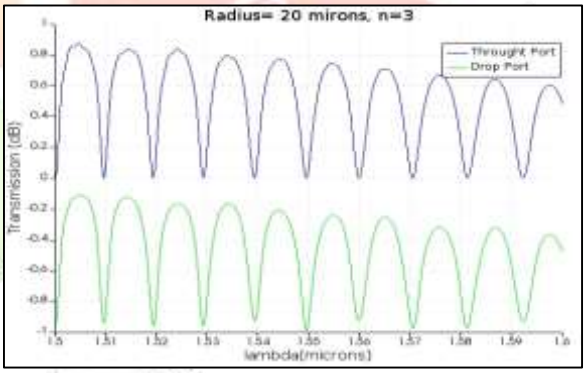


Fig. 12 Transmission plot for radius 20 μm and index=3

The above graphs are the output plot at through and drop port of the micro ring resonator. The graph is plotted between normalized power and wavelength. Using these graphs, the various parameters of the ring resonator can be evaluated which will descried the performance analysis of micro ring resonator.

The FSR behavior of the ring resonator is shown in the table 2 and Fig. 13. The analysis result shows that the FSR is significantly dependent on the size of the ring, i.e., The FSR for the radius 2 μm is 90.05 nm, while for 8 μm it is 24.67 nm and for 20 μm FSR value is 9.77 nm. The highest FSR value is obtained in the case where the radius is 2 μm while the lowest at 20 μm.

Table 2. Calculation of FSR for index=3

| Radius (µm) | Calculation for FSR | FSR (nm) |
|---|---|---|
| 2 | 1.50888-1.59893 | 90.05 |
| 4 | 1.58266-1.53048 | 52.18 |
| 5 | 1.58183-1.53953 | 42.3 |
| 6 | 1.54669-1.51308 | 33.61 |
| 8 | 1.53165-1.50698 | 24.67 |
| 10 | 1.54409-1.52386 | 20.33 |
| 15 | 1.53401-1.52057 | 13.44 |
| 20 | 1.51941-1.50964 | 9.77 |

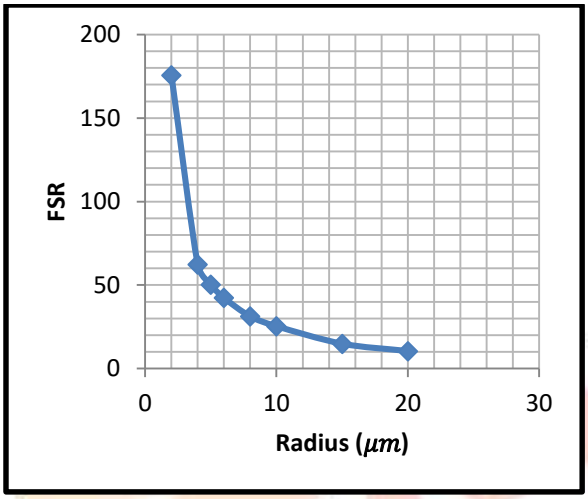


Fig. 13 Variation of FSR with increasing radius for index 3

The FWHM behavior of the ring resonator is shown in the table 3 and Fig. 14. The analysis result shows that the FWHM is significantly dependent on the size of the ring, i.e., The FWHM for the radius 2 µm is 18 nm, while for 8 µm it is 5.2 nm and for 20 µm FSR value is 3.81 nm. The highest FWHM value is obtained in the radius of 2 µm while the lowest at 20 µm.

Table 3 Calculation of FSR for index=3

| Radius (µm) | Calculation for FWHM | FWHM (µm) |
|---|---|---|
| 2 | 1.53108-1.51308 | 18 |
| 4 | 1.53616-1.52216 | 14 |
| 5 | 1.5422-1.53342 | 8.78 |
| 6 | 1.55071-1.5437 | 7.01 |
| 8 | 1.51313-1.50793 | 5.2 |
| 10 | 1.511-1.50604 | 4.96 |
| 15 | 1.50976-1.50566 | 4.1 |
| 20 | 1.51457-1.51076 | 3.81 |

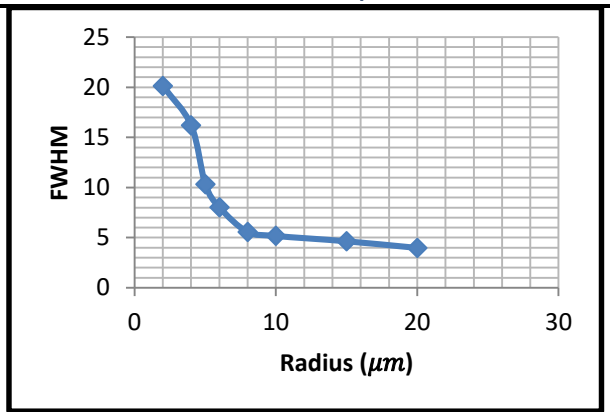


Fig. 14 Variation of FWHM with increasing radius for index 3

Table 4 Calculation of Q-Factor for index=3

| Radius (μm) | Calculation for Q-Factor | Q-Factor |
|---|---|---|
| 2 | 1500/18 | 83.3 |
| 4 | 1500/14 | 107.1 |
| 5 | 1500/8.78 | 170.8 |
| 6 | 1500/7.01 | 213.9 |
| 8 | 1500/5.2 | 288 |
| 10 | 1500/4.96 | 304.8 |
| 15 | 1500/4.1 | 365.8 |
| 20 | 1500/3.81 | 393.7 |

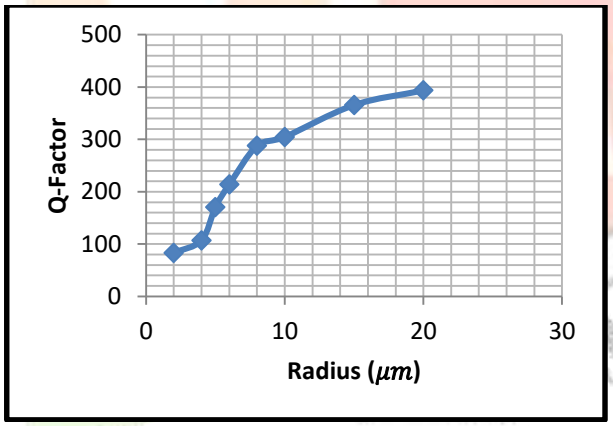


Fig. 15 Variation of Q-Factor with increasing radius for index 3

For the calculation of Q-factor, 1500 nm is taken as the resonant wavelength. The Q-Factor behavior of the ring resonator is shown in the table 4 and Fig. 15. The analysis result shows that the Q-Factor is significantly dependent on the size of the ring, i.e., the highest q factor achieved at the radius of 2 μm and the lowest Q-factor is achieved at 20 μm.

## V. Conclusion

In this paper, we observed that the ring size has significant impact on the quality of the device. For group index 3 and resonant wavelength of 1500 μm, the quality factor for a 2 μm ring radius is about 83.3 whereas for a 20 μm radius that is about 393.7. For a ring size of 2 μm the value of FSR is about 90.05 nm , which is about only 9.77 nm for a ring resonator with radius of 20 μm. It is seen that the ring size has significant impact on the quality of the device and for better performance and also FSR and FWHM measurement is same for both through and drop ports. It can be concluded that with the increasing radius FSR and FWHM decreases and with increasing radius Q-factor increases for single micro ring resonator.

## REFERENCES


[1] Uddin, M.R. et. al. (2016).Quality analysis of a photonic micro-ring resonator. In 2016 international conference on computer and communication engineering (ICCCE) (pp. 382-385). IEEE.

[2] Bogaerts, W., et. al. (2012). Silicon microring resonators. Laser & Photonics Reviews, 6(1), pp.47-73.

[3] Bogaerts, W., et. al. (2006).Compact wavelength-selective functions in silicon-on-insulator photonic wires. IEEE Journal of Selected Topics in Quantum Electronics, 12(6), pp.1394-1401.

[4] Heebner, J.E. and Boyd, R.W., 1999. Enhanced all-optical switching by use of a nonlinear fiber ring resonator. Optics letters, 24(12), pp.847-849.

[5] Kedia, J. and Gupta, N., 2015. An FDTD analysis of serially coupled double ring resonator for DWDM. Optik, 126(24), pp.5641-5644.

[6] Manolatou, C., Khan, M.J., Fan, S., Villeneuve, P.R., Haus, H.A. and Joannopoulos, J.D., 1999. Coupling of modes analysis of resonant channel add-drop filters. IEEE journal of quantum electronics, 35(9), pp.1322-1331.

[7] Raad, B.A. and Jacobs, I., 1992. Tunneling through a total internal reflection layer. IEEE transactions on education, 35(2), pp.112-114.

[8] Choi, J.M., Lee, R.K. and Yariv, A., 2001. Control of critical coupling in a ring resonator–fiber configuration: application to wavelength-selective switching, modulation, amplification, and oscillation. Optics letters, 26(16), pp.1236-1238.

[9] Cai, M., Painter, O. and Vahala, K.J., 2000. Observation of critical coupling in a fiber taper to a silica-microsphere whispering-gallery mode system. Physical review letters, 85(1), p.74.

[10] Notomi, M., Shinya, A., Mitsugi, S., Kuramochi, E. and Ryu, H.Y., 2004. Waveguides, resonators and their coupled elements in photonic crystal slabs. Optics express, 12(8), pp.1551-1561.

[11] Bogaerts, W., Dumon, P., Van Thourhout, D., Taillaert, D., Jaenen, P., Wouters, J., Beckx, S., Wiaux, V. and Baets, R.G., 2006. Compact wavelength-selective functions in silicon-on-insulator photonic wires. IEEE Journal of Selected Topics in Quantum Electronics, 12(6), pp.1394-1401.

[12] Tsang, H.K. and Liu, Y., 2008. Nonlinear optical properties of silicon waveguides. Semiconductor Science and Technology, 23(6), p.064007.

[13] Cardenas, J., Foster, M.A., Sherwood-Droz, N., Poitras, C.B., Lira, H.L., Zhang, B., Gaeta, A.L., Khurgin, J.B., Morton, P. and Lipson, M., 2010. Wide-bandwidth continuously tunable optical delay line using silicon microring resonators. Optics express, 18(25), pp.26525-26534.

[14] Bogaerts, W., De Heyn, P., Van Vaerenbergh, T., De Vos, K., Kumar Selvaraja, S., Claes, T., Dumon, P., Bienstman, P., Van Thourhout, D. and Baets, R., 2012. Silicon microring resonators. Laser & Photonics Reviews, 6(1), pp.47-73.

[15] Fazacas, A. and Sterian, P., 2012. Finite-Difference Time-Domain Method (FDTD) used to simulate Micro-ring resonator for student applications. Journal of Optoelectronics and Advanced Materials, 14(3-4), pp.344-349.

[16] Zhang, Y., Zhang, X., Liu, X. and Yuan, P., 2013, December. Coupled add-drop ring resonator for highly sensitive sensing. In 2013 Seventh International Conference on Sensing Technology (ICST) (pp. 365-368). IEEE.

[17] Yan, S., Li, M., Luo, L., Ma, K., Xue, C. and Zhang, W., 2015. Optimisation design of coupling region based on SOI micro-ring resonator. Micromachines, 6(1), pp.151-159.

[18] Uddin, M.R., Siang, T.K., Munarah, N., Norfauzi, M., Ahmed, N. and Salam, M.A., 2016, July. Quality analysis of a photonic micro-ring resonator. In 2016 international conference on computer and communication engineering (ICCCE) (pp. 382-385). IEEE.

[19] Li, A., Huang, Q. and Bogaerts, W., 2016. Design of a single all-silicon ring resonator with a 150 nm free spectral range and a 100 nm tuning range around 1550 nm. Photonics Research, 4(2), pp.84-92.

[20] Neunzert, A. A. M.(2019 ) Gravitational Waves From Spinning Neutron Stars: Development of a Directed Binary Search Technique and Spectral Characterization Tools, dissertation of Doctor of Philosophy (Physics) in The University of Michiga.

[21] Lumerical FDTD Mode Solution Tool

[22] Singh, K., Mandal, S. Design and performance analysis of all-optical 1:4 and 1:8 high speed demultiplexer using InGaAsP–InP optical microring resonator in Z-domain. Opt Quant Electron 51, 252 (2019).

[23] Madsen, C.K., Zhao, J.: Optical Filter Design and Analysis: A Signal Processing Approach. Wiley, New York (1999)